

*Supporting Information*

**Cross-linking Enhances the Performance of Four-electron Carbonylpyridinium Based Polymers for Lithium Organic Batteries**

*Hongyan Li, Ling Chen, Fangfang Xing, Hongya Miao, Jing Zeng, Sen Zhang, Xiaoming He\**

\*To whom correspondence should be addressed

Key Laboratory of Applied Surface and Colloid Chemistry (Ministry of Education), School of Chemistry and Chemical Engineering, Shaanxi Normal University, Xi'an 710119, P.R. China

\*Corresponding Author Email: xmhe@snnu.edu.cn

## 1. Materials

4-Bromopyridine hydrochlorides, potassium carbonate, *n*-butyl lithium (2.5 M in *n*-hexane) were purchased from Sinopharm Chemical Reagent Co., Adamas or Alfa Aesar. Poly(vinylidene fluoride) (PVDF,  $M_w = 534\ 000$ ), N-methylpyrrolidone (NMP), Super P were obtained from Shenzhen Kejing Zhida Technology Co., Ltd. The lithium chip, CR2032 battery case, 2.0 mol L<sup>-1</sup> LiClO<sub>4</sub> in tetraglyme (G4), carbon paper and separator (Celgard2400) were purchased from DoDoChem. PVDF and Ketjen Black (ECP-600JD) were dried at 80 °C for 12 h under vacuum oven before use. All other reagents or solvents were used without further purification, unless indicated otherwise.

## 2. Instruments

<sup>1</sup>H NMR and <sup>13</sup>C NMR spectra were obtained on 600 MHz BRUKER spectrometer. Mass spectrometry data were collected on a Bruker maxis UHR-TOF mass spectrometer in ESI positive mode. IR spectra were obtained on a PE-Frontier instrument. Cyclic voltammetry (CV) analyses were performed on a Shanghai Chenhua CHI760E instrument, with a polished glassy carbon electrode as the working electrode, a Pt-wire as counter electrode, and 0.01 M Ag/AgCl (3 M KCl) as a reference electrode. The UV-vis reflection spectra were obtained in solid state powder on an UV-vis spectrophotometer (UV-Lambda 950, PerkinElmer, US) equipped with an integrating sphere assembly, using BaSO<sub>4</sub> as a reflectance sample. Scanning electron microscope (SEM) images were recorded using a Hitachi SU8220 system. The morphology and structure of the obtained samples were identified using powder X-ray diffraction (XRD, Bruker D8 Advance with Cu-K $\alpha$  radiation). Thermogravimetric analysis (TGA) was performed under nitrogen atmosphere from 25 to 800 °C with a heating rate of 10 °C min<sup>-1</sup>. The X-ray photoelectron spectra (XPS) experiments were carried out on a PHI-5400

electron spectrometer.

### 3. Synthesis

**Synthesis of 4-Bromopyridine.** This was prepared following a protocol from the literature (N. Anwar, et al. *ACS Macro Lett.* **2013**, *2*, 766-769). 4-Bromopyridine hydrochlorides (6.8 g, 35 mmol) were added to the aqueous solution of potassium carbonate (14.5 g, 105 mmol), which was stirred for 10 min at 0 °C. Then the mixed solution was extracted with ethyl ether, and the organic phase was concentrated by evaporation under vacuum to obtain a colorless transparent oil (yield: 4.9 g, 90 %).

**Synthesis of 1,4-Phenylenebis(4-pyridylmethanone) (M1).** This was synthesized according to a modified procedure from the literature (F. L. Minn, et al. *J. Am. Chem. Soc.* **1970**, *92*, 3600–3610). In a flame-dried Schlenk flask under nitrogen atmosphere, 4-bromopyridine (4.74 g, 30 mmol) was dissolved in dry ethyl ether (100 mL) and cooled to -78 °C. *n*-butyl lithium (2.5 M, 14.4 mL, 36 mmol) in hexane was added dropwise, and the mixture was stirred at -78 °C for 1 h. Then a solution of 1,4-dicyanobenzene (1.54 g, 12 mmol) in dry THF (80 mL) was added. The mixture was stirred at -78 °C for 1 h, and slowly allowed to warm to room temperature for 2 h. Then 10 % H<sub>2</sub>SO<sub>4</sub> (100 mL) was added and the mixture was stirred for 2 h at room temperature, followed by removal of organic volatiles by evaporation under vacuum. After that, the solution was made basic by addition of 1 M KOH and extracted with CH<sub>2</sub>Cl<sub>2</sub>, dried with anhydrous MgSO<sub>4</sub>. Finally, the organic phase was concentrated by evaporation under vacuum and the solid was precipitated in petroleum ether, filtered and dried to obtain the product as yellow solids (yield: 2.1 g, 61.4 %). <sup>1</sup>H NMR (600 MHz, DMSO-*d*<sub>6</sub>): δ/ppm = 8.86 (d, *J* = 6.0 Hz, 4H), 7.96 (s, 4H), 7.68 (d, *J* = 6.0 Hz, 4H). <sup>13</sup>C NMR (600 MHz, DMSO-*d*<sub>6</sub>): δ/ppm =

194.93, 150.96, 143.64, 139.56, 130.53, 123.13. HR-MS:  $m/z$  calculated for  $C_{18}H_{13}N_2O_2$  289.0972, found 289.0975.

**Synthesis of N,N'-Dibenzyl-(1,4-phenylene)-(4,4'-dicarbonyl-bispyridinium) dibromide (M2).** A mixture of **M1** (144 mg, 0.5 mmol) and benzyl bromide (855 mg, 0.6 mL, 10 mmol) in DMF (1.5 mL) were stirred at 90 °C for 24 h under nitrogen atmosphere. After being cooled to room temperature, the mixture was filtered and the residue was washed with ethyl ether to afford the pure product as pink solids (yield: 202 mg, 64 %).  $^1H$  NMR (600 MHz, DMSO- $d_6$ ):  $\delta/ppm$  = 9.45 (d,  $J$  = 7.2 Hz, 4H), 8.41 (d,  $J$  = 7.2 Hz, 4H), 8.03 (s, 4H), 7.61 (d,  $J$  = 6.6 Hz, 4H), 7.49 (m, 6H), 5.99 (s, 4H).  $^{13}C$  NMR (600 MHz, DMSO- $d_6$ ):  $\delta/ppm$  = 191.97, 150.99, 146.39, 138.70, 134.43, 131.01, 129.99, 129.72, 129.58, 128.14, 63.93. HR-MS:  $m/z$  calculated for  $C_{32}H_{26}N_2O_2^{2+}$  [M-2Br] $^{2+}$  235.0992, found 235.0999.

**Synthesis of DBMP.** A mixture of **M1** (576.6 mg, 2.0 mmol) and  $\alpha,\alpha'$ -dibromo-*p*-xylene (528 mg, 2.0 mmol) in dry DMF (40 mL) was heated at 90 °C for three days under nitrogen. After that, benzyl bromide (855 mg, 0.6 mL, 10 mmol) was added, and the reaction was stirred at 90 °C for 24 h for end-capping of some unreacted pyridines. The product was isolated by centrifugation and washed several times with DMF, THF and  $CH_2Cl_2$  to afford a brown solid (yield: 938 mg, 88 %).

**Synthesis of TBMP.** The procedure was similar to that used to prepare **DBMP**, except that 1,3,5-tris(bromomethyl)benzene (357 mg, 1.0 mmol) was used instead of  $\alpha,\alpha'$ -dibromo-*p*-xylene. The product was isolated as a reddish brown solid (yield: 663 mg, 84 %).

**Determination of the degree of polymerization (DP) of DBMP.** **DBMP** (1.0 mmol) and methyl trifluoromethanesulfonate (10 mol) were stirred at RT overnight in 30 mL dry  $CH_3CN$  under nitrogen

condition. After removing the solvent by evaporation, the product was washed several times with CH<sub>2</sub>Cl<sub>2</sub> to afford **DBMP** (OTf). The anion metathesis not only enhance the solubility of polymer, but also end-cap the unreacted N site with methyl group. Based on the integration aromatic signal and characteristic (N<sup>+</sup>)-CH<sub>3</sub> at the end, the DP of polymer could be determined to be 13 (Figure S7).

#### 4. Battery Fabrication and Testing

**DBMP** and **TBMP** working electrode materials were prepared by mixing the **DBMP** or **TBMP**, Ketjen Black (ECP-600JD) and PVDF with a mass ratio of 4/4/2 (unless other noted) using NMP as dispersion solvent. Then the slurry was coated on the carbon paper with a diameter of 12 mm and the mass loading of the active materials was *ca.* 0.7 mg cm<sup>-2</sup>. The fully prepared electrodes were then dried at 80 °C overnight in a vacuum oven in order to remove any residual solvent. Assembly of the CR2032-type coin-type half cells were carried out in argon-filled glove box (<0.01 ppm of oxygen and water), with lithium metal as the anode, polypropylene separator film (Celgard2400) as the separator, and 2.0 mol L<sup>-1</sup> LiClO<sub>4</sub> in tetraglyme (G4) as the electrolyte. The CV and EIS tests were performed on CHI760E electrochemical working station, and the charge-discharge curves were conducted on LAND CT2001A at 30 °C, unless otherwise noted.

#### 5. Calculations of the Electrochemical Metrics

Theoretical capacity ( $C_{\text{theor}}$ , mAh g<sup>-1</sup>) was calculated according to the equation (1):

$$C_{\text{theor}} = \frac{nF}{3.6 \times M} \quad (1)$$

where  $n$  is the number of electrons transferred per molecules,  $F$  is the Faraday's constant (96484 C mol<sup>-1</sup>),  $M$  is molecular weight of the molecules.

The  $b$ -value and capacitive contribution at a particular potential were determined as follows:

The relationship between scan rate ( $v$ ,  $\text{mV s}^{-1}$ ) in a CV and the corresponding cathodic or anodic peak current ( $i_p$ ,  $\text{A g}^{-1}$ ) is shown in equation (2).<sup>S1</sup> The  $b$ -value was the slope of the  $\log(v)$ - $\log(i_p)$  plots according to equation (3).

$$i_p = av^b \quad (2)$$

$$\log(i_p) = \log(a) + b \log(v) \quad (3)$$

where  $a$  and  $b$  are adjustable parameters.

Moreover, the relationship between the current at a particular potential ( $i(V)$ ,  $\text{A g}^{-1}$ ) and the scan rate ( $v$ ,  $\text{mV s}^{-1}$ ) is shown in equation (4).<sup>S2</sup> Solving for the values of  $k_1$  and  $k_2$  at each potential, we can obtain the percentage of capacitive contribution the total current ( $k_2v/i(V)$ ).

$$i(V) = k_1v^{1/2} + k_2v \quad (4)$$

## 6. Electronic conductivity calculation

Electronic conductivity ( $\sigma$ ,  $\text{S cm}^{-1}$ ) was calculated according to the equation (5):

$$\sigma = \frac{L}{R \times S} \quad (5)$$

where  $L$  (cm) is the thickness of the sheet,  $R$  ( $\Omega$ ) is the impedance of the sheet active material,  $S$  ( $\text{cm}^2$ ) is the surface area of the sheet. Conductivity was measured by linear scanning voltammetry (LSV). The polymer powders were pressed into sheets and then sandwiched between two electrodes for LSV test at  $100 \text{ mV s}^{-1}$ .

## 7. Calculation of apparent ion diffusion coefficients ( $D_{app}$ , $\text{cm}^2 \text{s}^{-1}$ ) from GITT

The apparent diffusion coefficients ( $D_{app}$ ) are calculated by the following equation: <sup>S3</sup>

$$D_{app} = \frac{4}{\pi\tau} \left( \frac{V_m m_B}{SM_m} \right)^2 \left( \frac{\Delta E_s}{\Delta E_t} \right)^2 \quad (6)$$

where  $D_{app}$  is the apparent ion diffusion coefficient ( $\text{cm}^2 \text{s}^{-1}$ ),  $\tau$  is the the duration of the current pulse (s),  $V_m$  is the molar volume of the active material ( $\text{cm}^3 \text{mol}^{-1}$ ),  $m_B$  is the mass of the active material in the electrolyte (g),  $M_m$  is the molar mass of active material ( $\text{g mol}^{-1}$ ),  $S$  is the contact surface area ( $\text{cm}^2$ ) between electrode and electrolyte,  $\Delta E_s$  is the equilibrium potential change induced by current pulse,  $\Delta E_t$  is the potential variation during the constant current pulse.

## 8. Supplementary Schemes, Figures and Tables

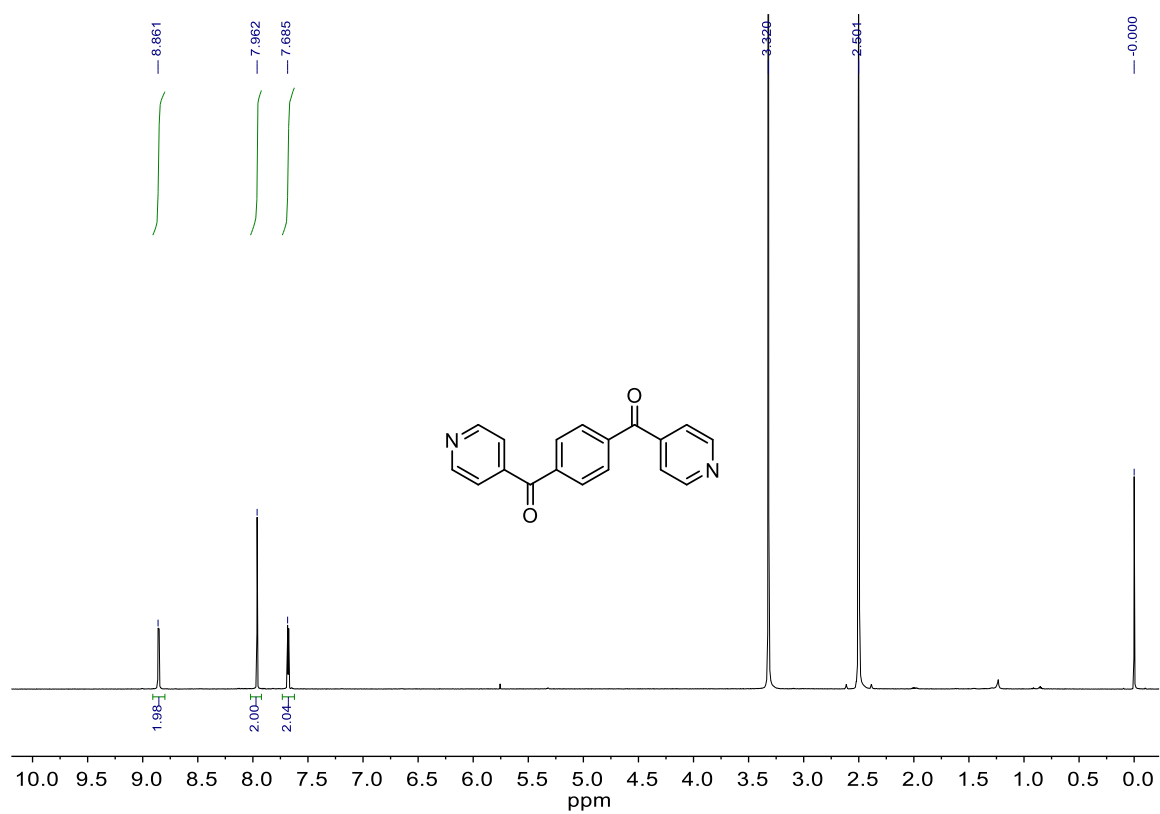


**Figure S1.**  $^1\text{H}$  NMR spectrum of **M1** in  $\text{DMSO-}d_6$ .



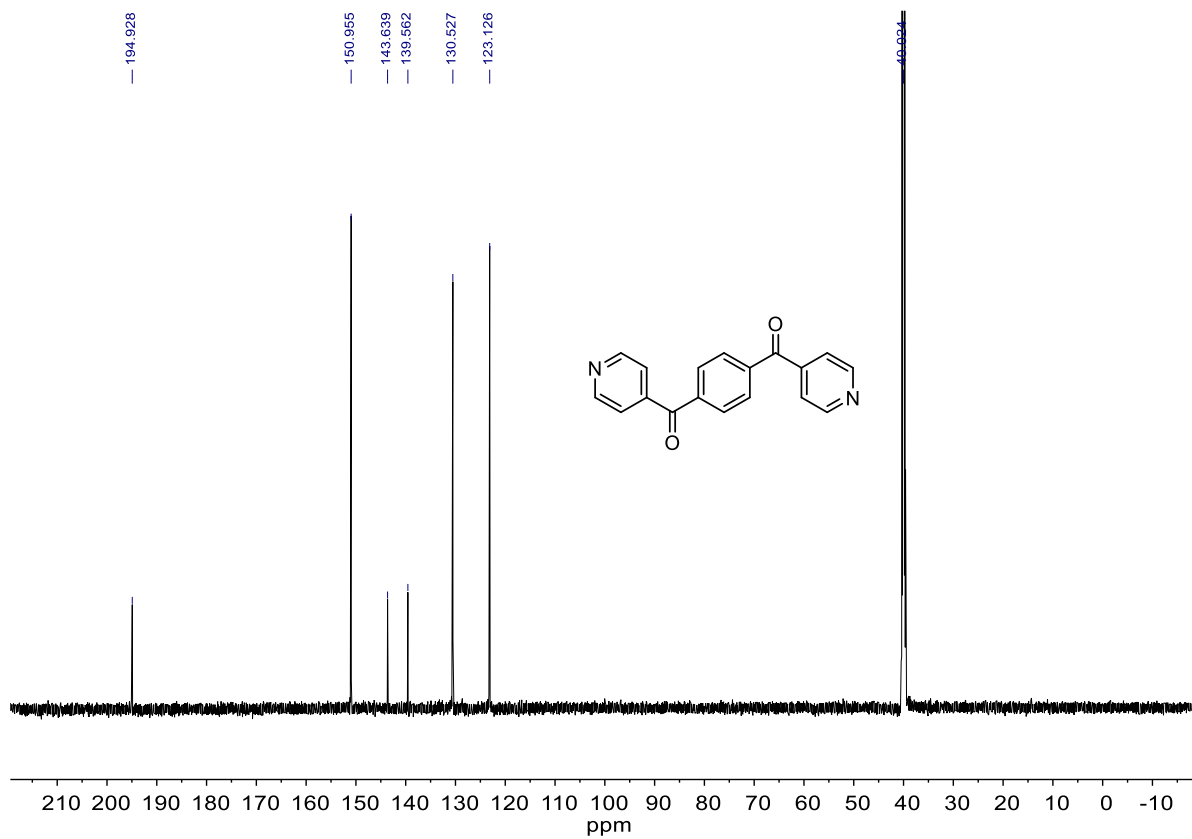


**Figure S2.**  $^{13}\text{C}$  NMR spectrum of M1 in  $\text{DMSO-}d_6$ .

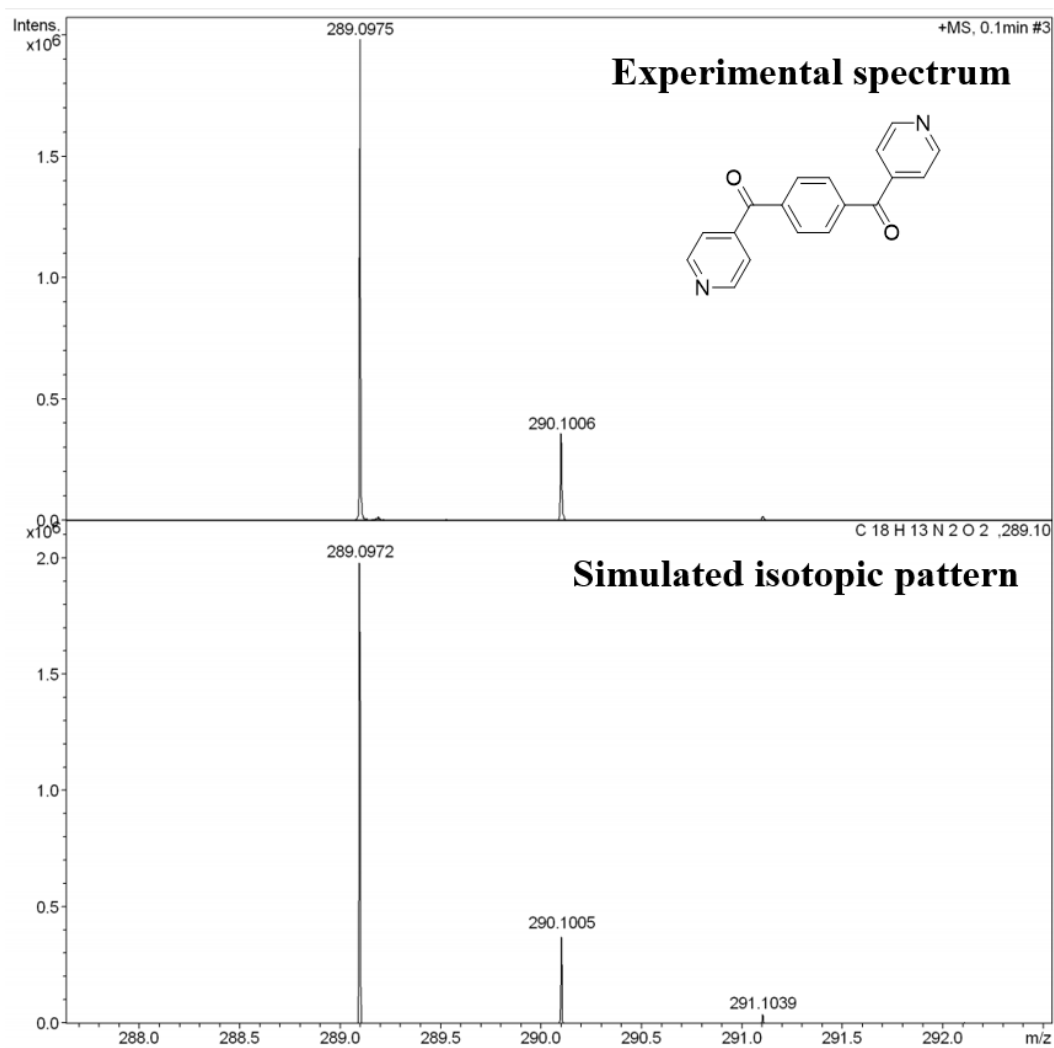


**Figure S3.** HR-MS spectrum of M1.

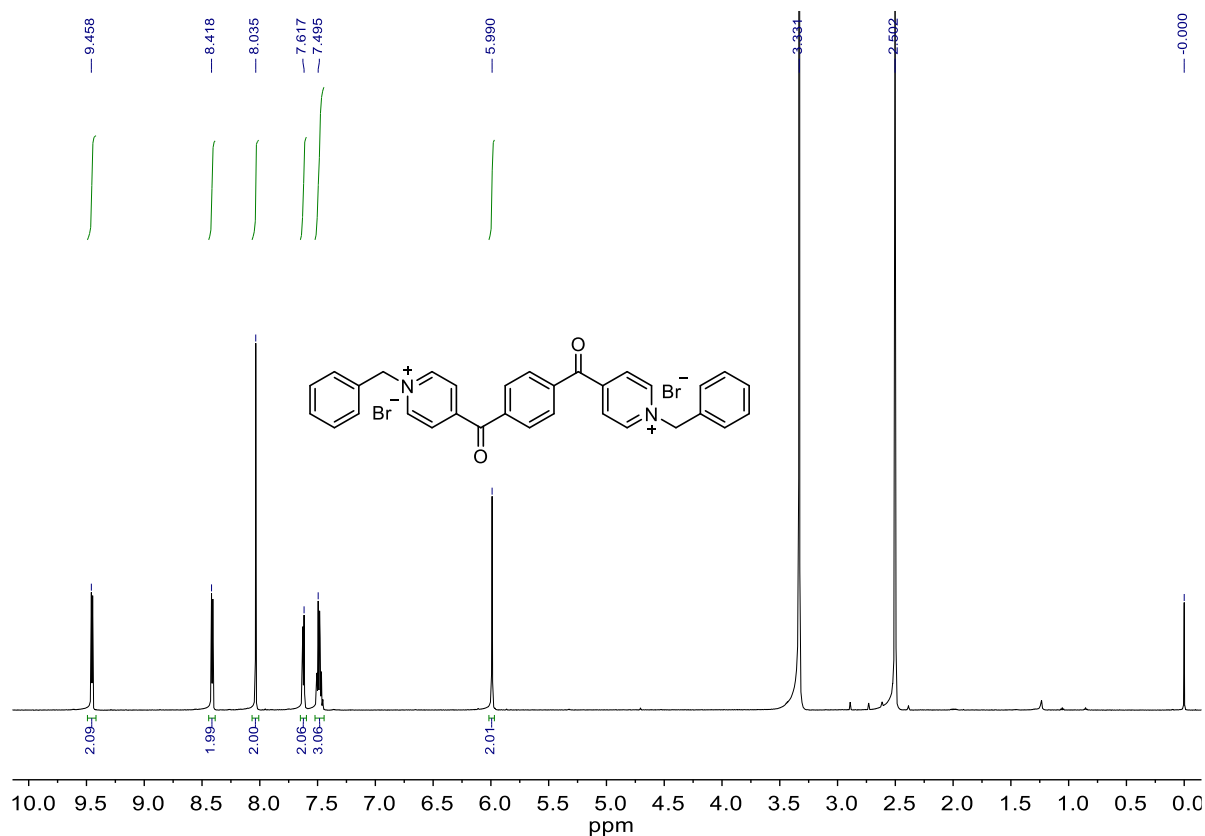


Figure S4.  $^1\text{H}$  NMR spectrum of M2 in  $\text{DMSO-}d_6$ .

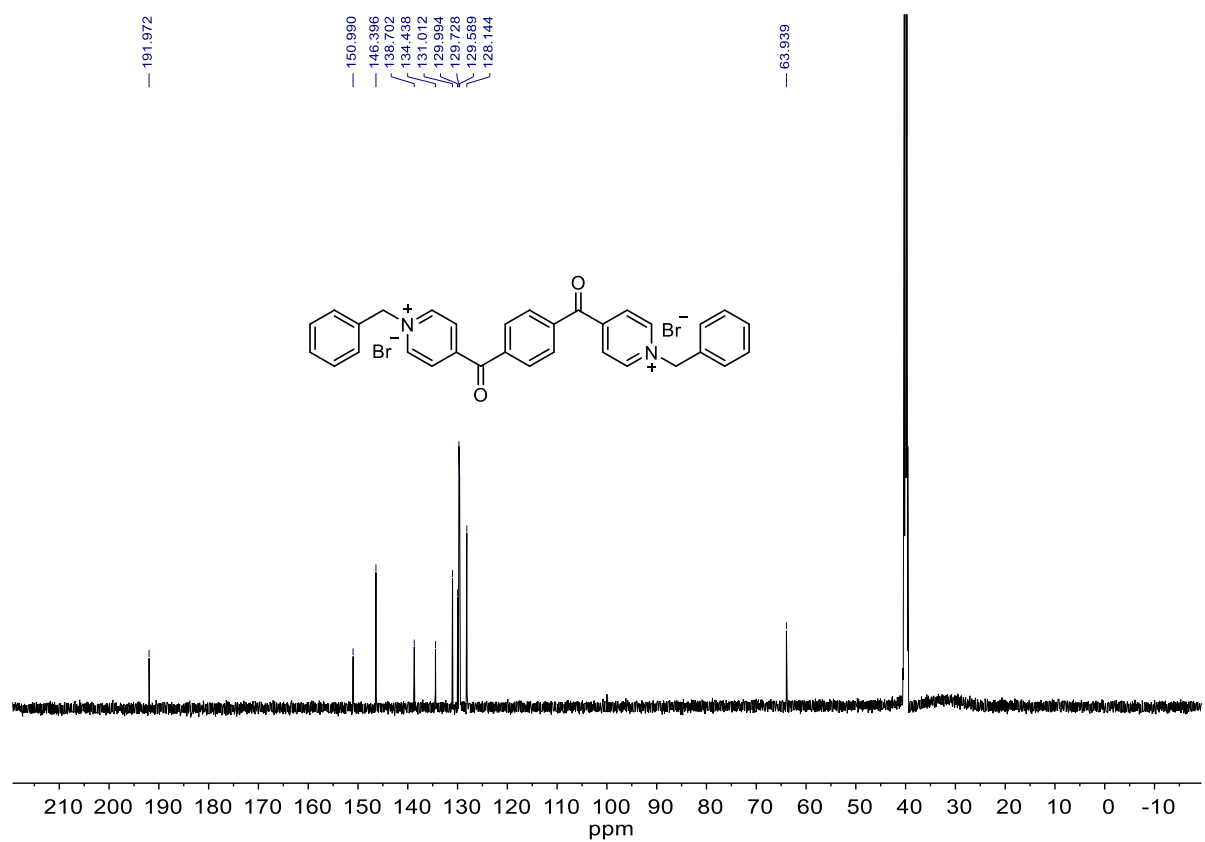
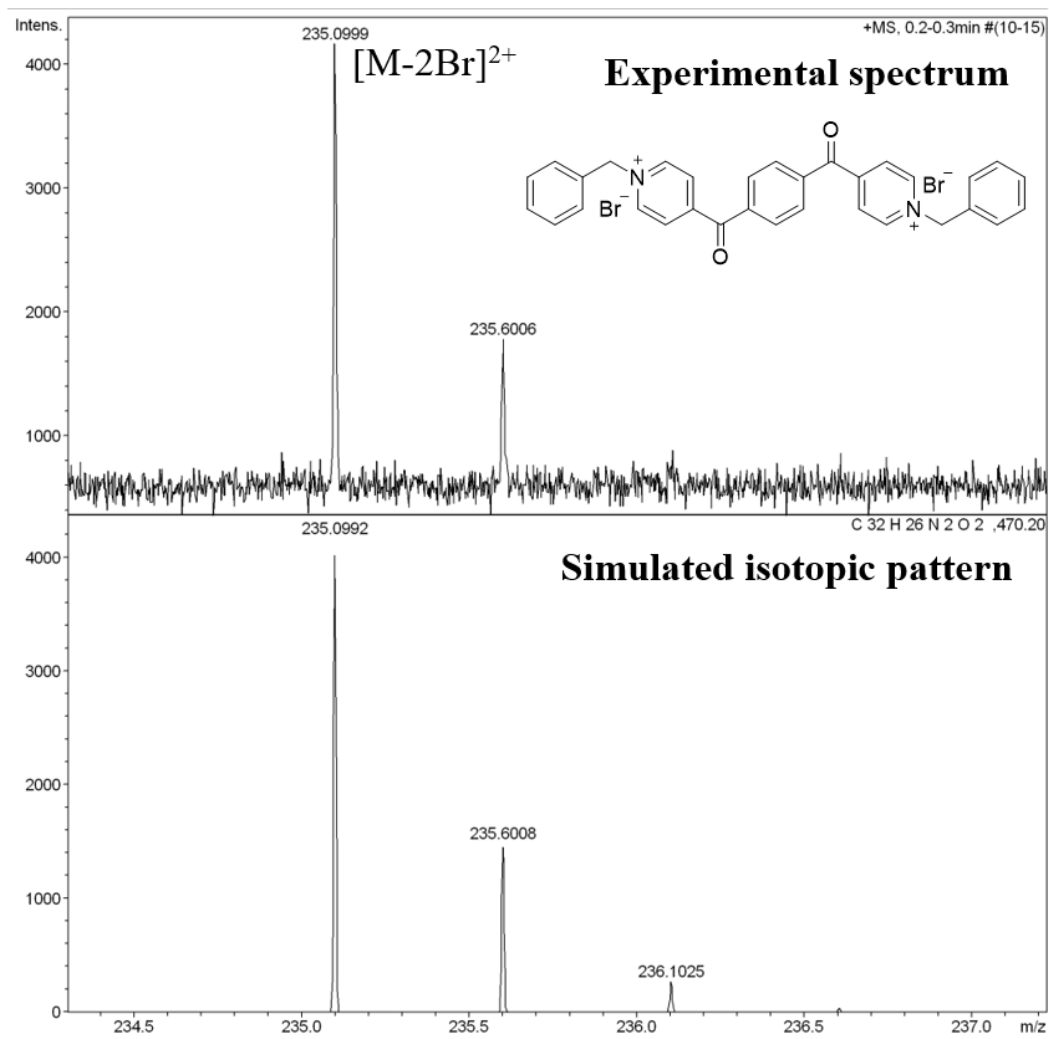
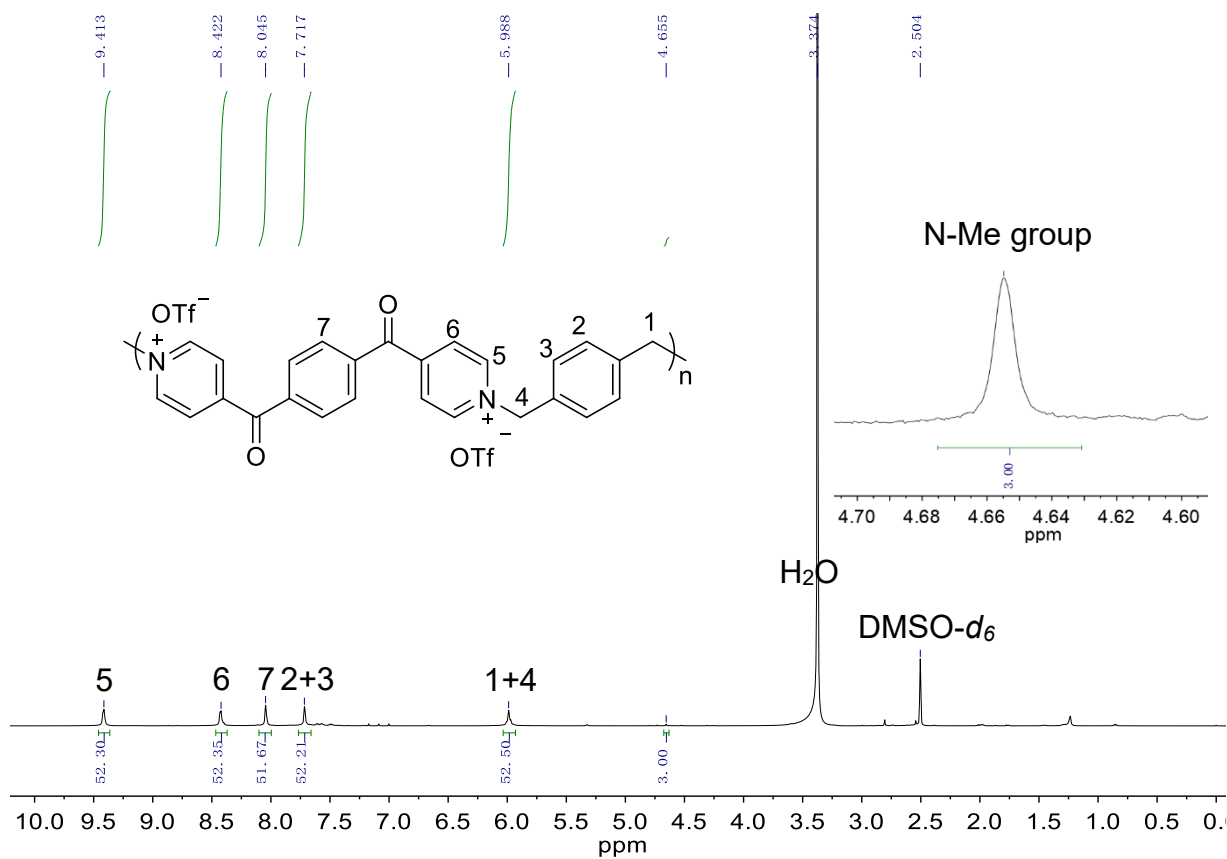


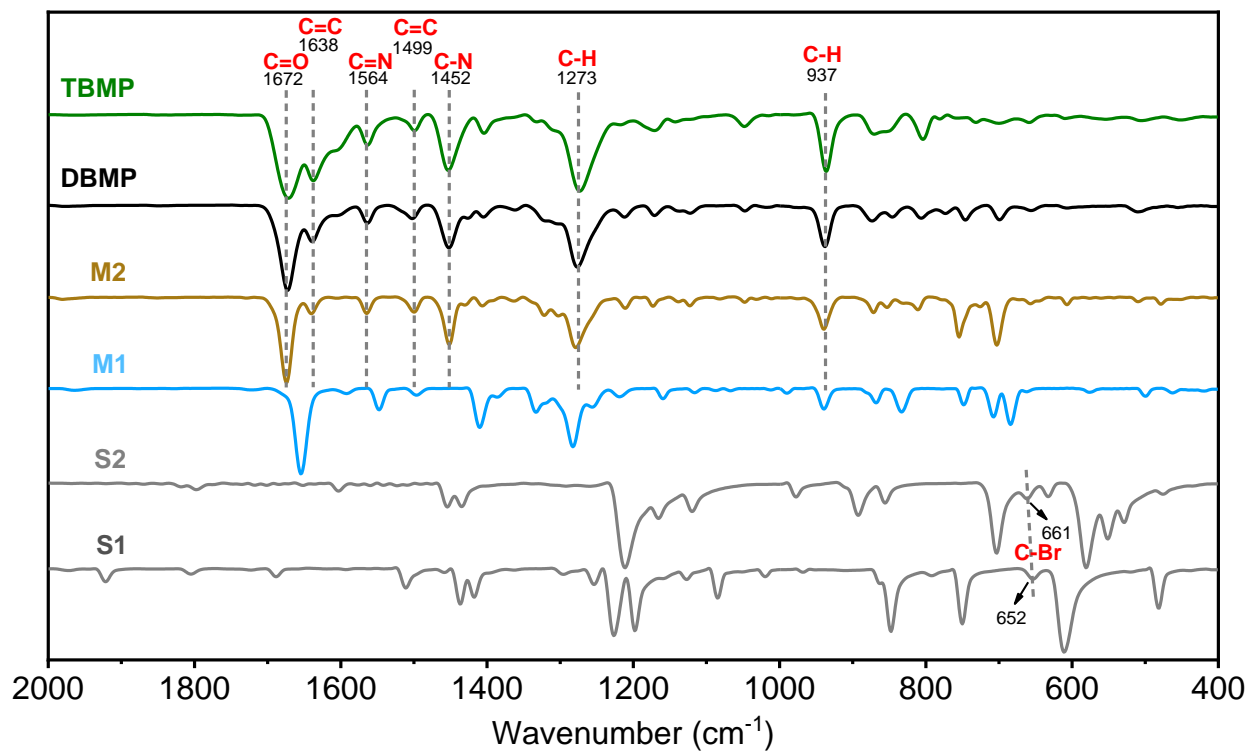
Figure S5.  $^{13}\text{C}$  NMR spectrum of M2 in  $\text{DMSO-}d_6$ .



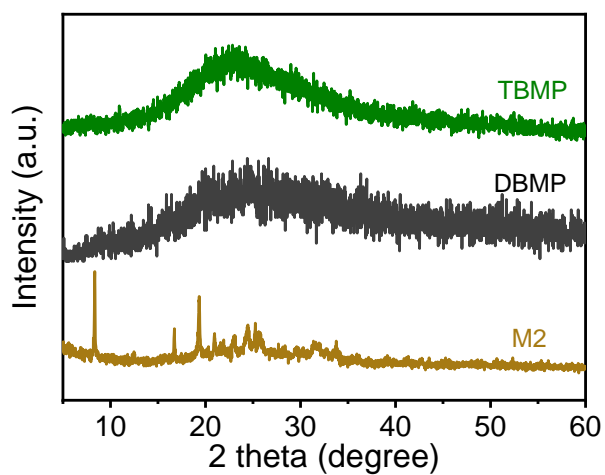
**Figure S6.** HR-MS spectrum of **M2**.



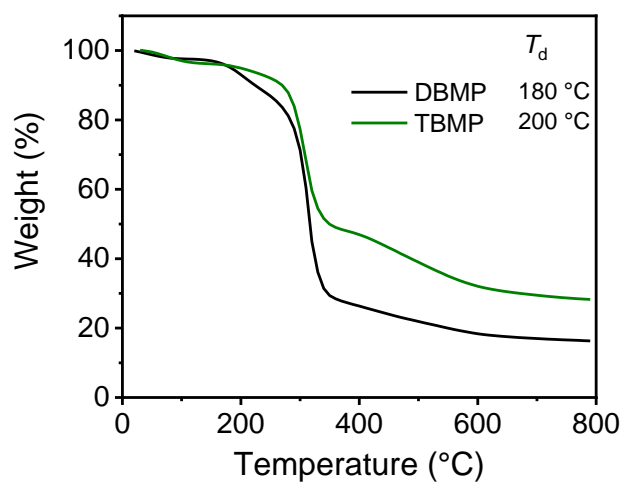
**Figure S7.**  $^1\text{H}$  NMR of DBMP(OTf) for determining the degree of polymerization (DP).



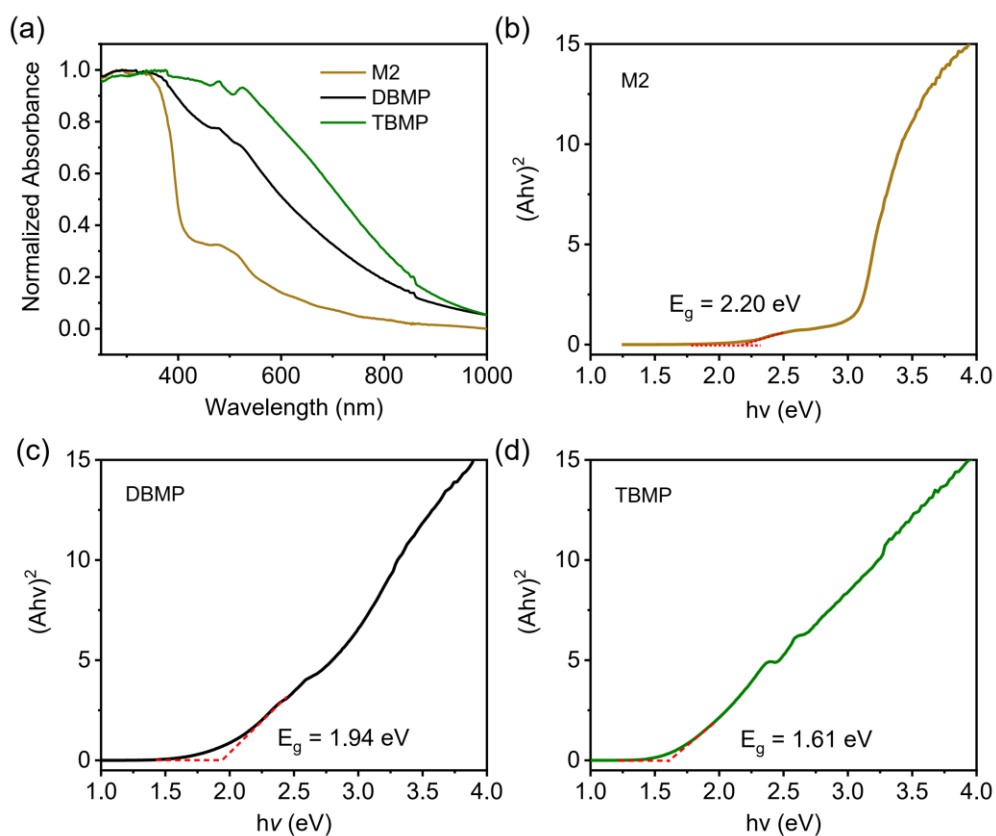
**Figure S8.** FT-IR spectra of S1, S2, M1, M2, DBMP and TBMP.



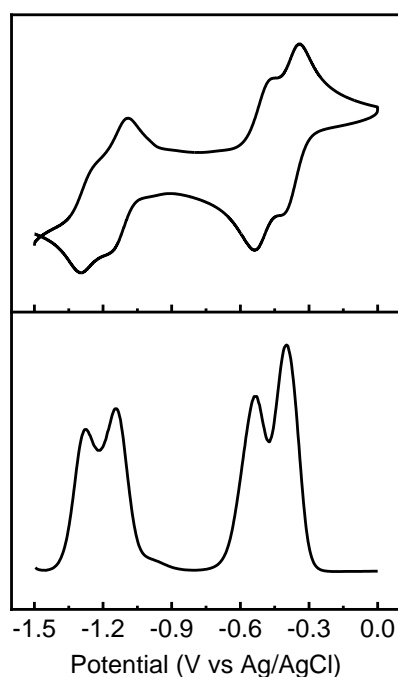
**Figure S9.** XRD spectra of M2, DBMP and TBMP.



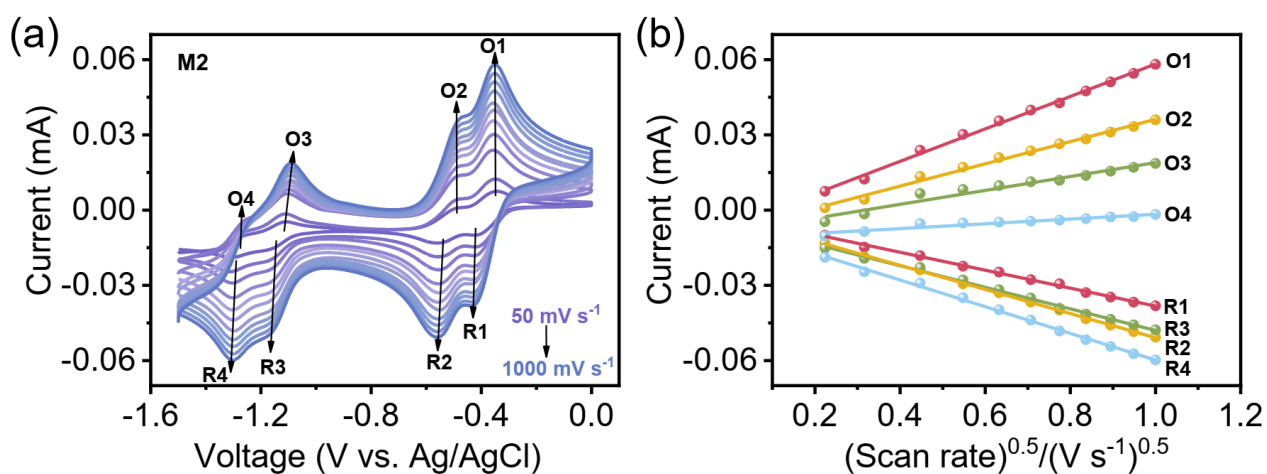
**Figure S10.** TGA curves of **DBMP** and **TBMP**.



**Figure S11.** (a) UV-vis spectra of **M2**, **DBMP** and **TBMP** in solid states, (b-d) corresponding Tauc plots for (b) **M2**, (c) **DBMP** and (d) **TBMP**. The intersection of two dashed lines indicates the value of optical band gap.

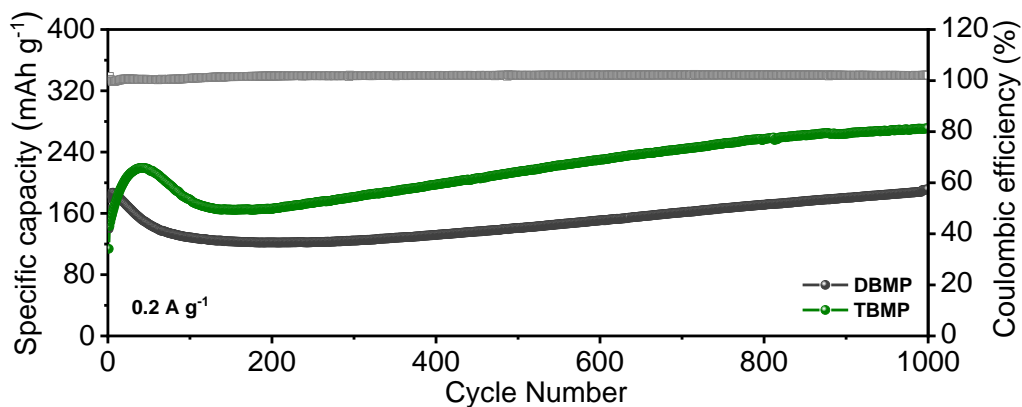


**Figure S12.** CV (top) and DPV (bottom) of **M2** in DMF solution ( $c = 1 \text{ mM}$ ) with  $0.1 \text{ M TBAPF}_6$  as the electrolyte. DPV parameters: Increase  $E = 4 \text{ mV}$ , amplitude =  $50 \text{ mV}$ , pulse width =  $60.0 \text{ ms}$ , sampling width =  $20.0 \text{ ms}$ , pulse period =  $500.0 \text{ ms}$ . The redox pair of  $\text{Br}^-$  counter-anion was not shown in the current potential range ( $-1.5$  to  $0 \text{ V}$ ).

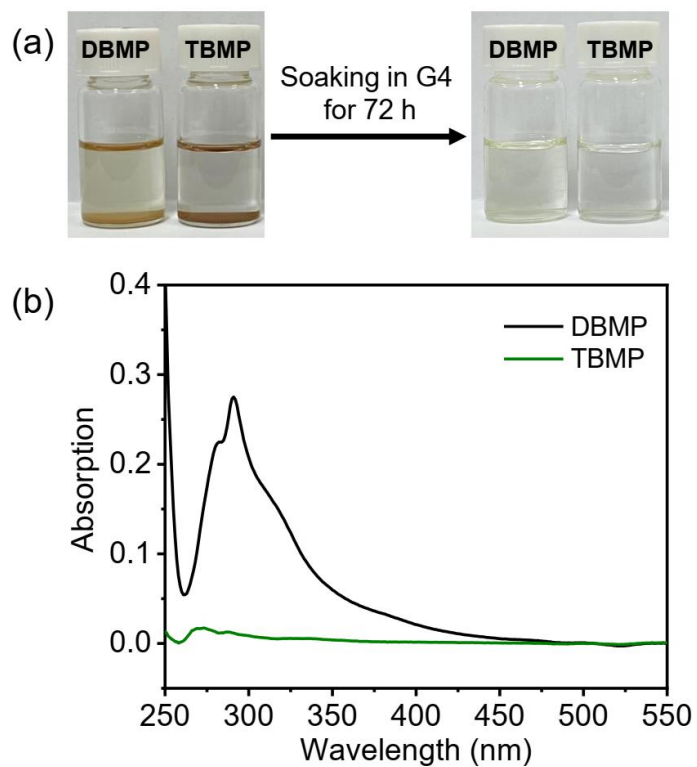


**Figure S13.** (a) Cyclic voltammograms of **M2** ( $1 \text{ mM}$ ) in DMF solution at varying scan rates ( $50$ - $1000 \text{ mV s}^{-1}$ ; peak height increases with increasing scan rate).  $\text{TBAPF}_6$  ( $0.1 \text{ M}$ ) was used as supporting electrolyte. (b) Linear plots of peak current vs. square root of the scan rate.

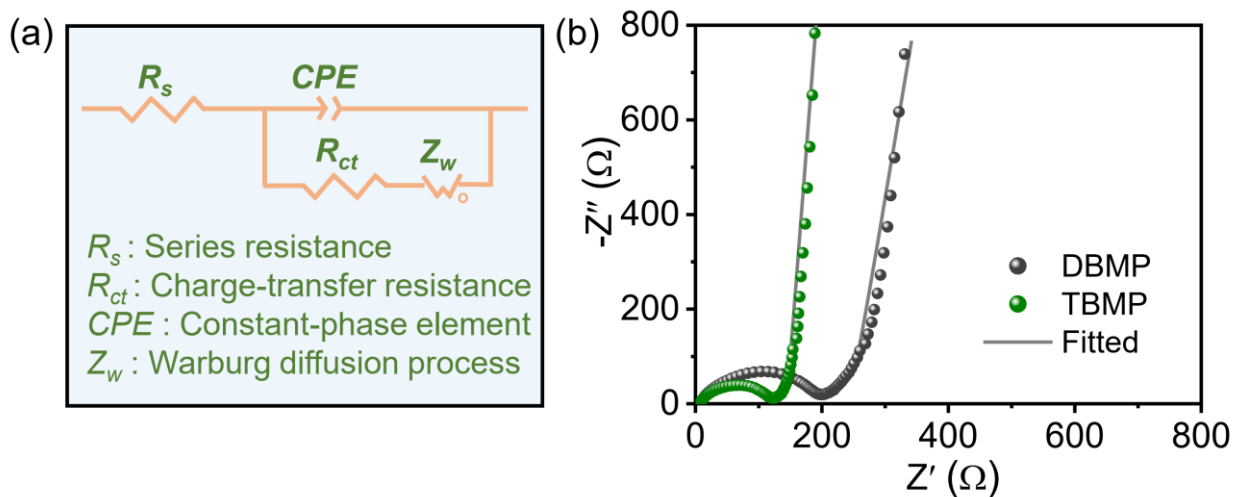




**Figure S14.** Cycling performance and Coulombic efficiency of **DBMP** and **TBMP** at 0.2 A g<sup>-1</sup>.

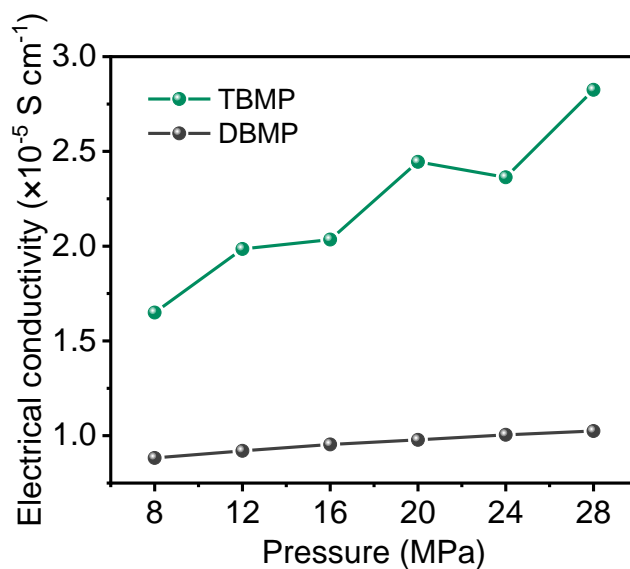


**Figure S15.** Solubility test in G4. (a) The photographs of **DBMP** and **TBMP** in G4 electrolyte and the corresponding filtrates, (b) the UV-vis spectra of the filtrates.



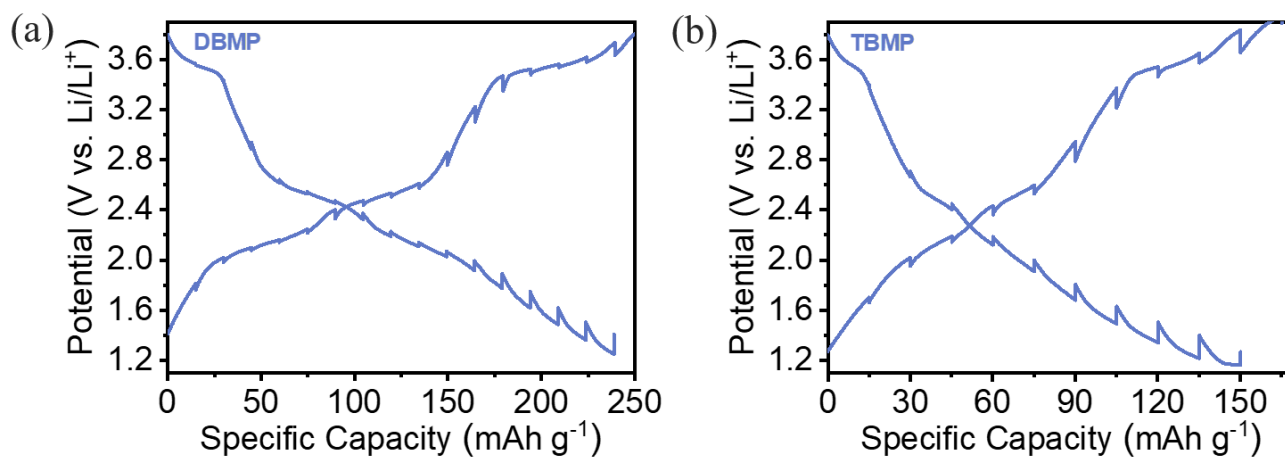
**Figure S16.** (a) The equivalent circuit for EIS analysis. (b) Nyquist plots of **DBMP** and **TBMP** based electrodes.

*Discussion:* **TBMP**-based electrodes showed a lower charge-transport resistance ( $R_{ct}$ ) of 120 Ω, compared to **DBMP** (200 Ω). This data confirms the better electronic conductivity of **TBMP**.

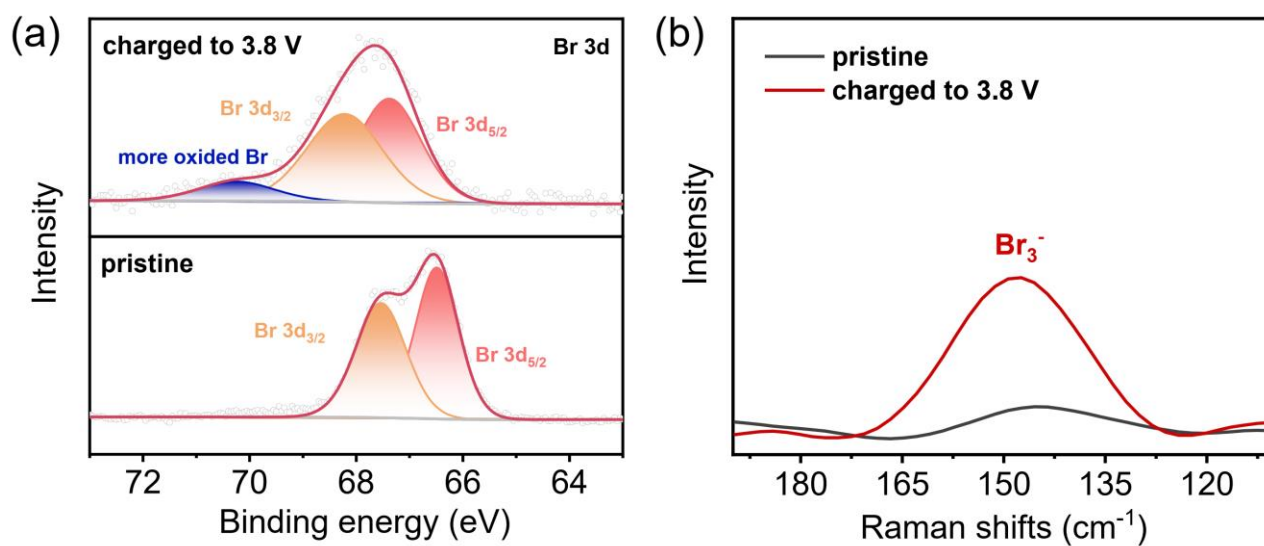


**Figure S17.** The electronic conductivity measurement of the **DBMP** and **TBMP** powder by a four-probe system. The powder was pressed into uniform pellets with a diameter of 12 mm and a thickness of 1 mm.

*Discussion:* The measured conductivity values by four-probe system are higher than those obtained by *I-V* curve with two-point probe. One possible reason is that the high-pressure condition can enhance the charge transfer from  $\text{Br}^-$  to carbonylpyridinium and increase the conductivity. However, the electronic conductivity trend of  $\text{TBMP} > \text{DBMP}$  is the same, given by two techniques.



**Figure S18.** GITT curves of **DBMP** and **TBMP** based electrodes at a current density of  $0.05 \text{ A g}^{-1}$ .

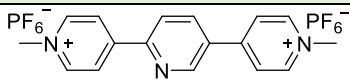
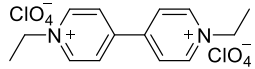
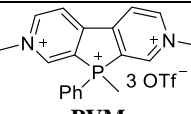
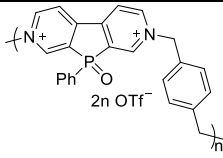
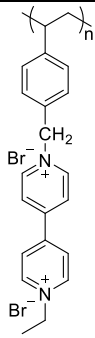


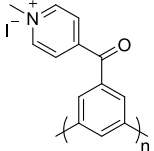
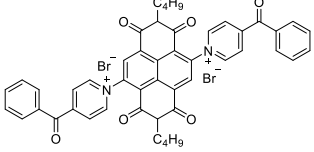
**Figure S19.** (a) *Ex-situ* Br 3d XPS spectra and (b) *ex-situ* Raman spectra of the **TBMP** electrode recorded at fresh state and charged to 3.8 V.

**Table S1.** Summary of the half-cell LOB results based on **DBMP** and **TBMP** electrodes.

| Compounds   | Theoretical $e$ numbers | $C_{\text{theor}}$ (mAh g <sup>-1</sup> ) | Rate Performance:<br>Capacity (mAh g <sup>-1</sup> )<br>Current density (A g <sup>-1</sup> ) | Cycle Stability:<br>Capacity (mAh g <sup>-1</sup> ) / Cycles / Current density (A g <sup>-1</sup> ) / percentage of $C_{\text{thero}}$ |
|-------------|-------------------------|---|--|--|
| <b>DBMP</b> | 16/3                    | 259                                       | 188, 158, 132, 115, 101, 87<br>0.05, 0.1, 0.2, 0.5, 1.0, 2.0                                 | 191/1000/0.2/74%<br>157/4000/1.0/61%   |
| <b>TBMP</b> | 16/3                    | 272                                       | 196, 204, 190, 148, 122, 106<br>0.05, 0.1, 0.2, 0.5, 1.0, 2.0                                | 271/1000/0.2/99%<br>252/4000/1.0/93%   |

**Table S2.** Summary of other reported pyridinium-based organic electrodes in the literature for LOBs.

| Materials (reference)   | redox window (V) | $C_{\text{thero}}$ (mAh g <sup>-1</sup> ) | Specific capacity (mAh g <sup>-1</sup> ) (Current)             | Cycle Stability: Capacity(mAh g <sup>-1</sup> ) /Cycles / Current |
|---|------------------|---|--|---|
| <br><b>Extended viologen derivative-4</b><br><i>ChemSusChem</i> <b>2020</b> , <i>13</i> , 2379-2385.               | 1.2 – 3.5        | 97  | 65 (0.02 A g <sup>-1</sup> )                                   | 47/10/0.02 A g <sup>-1</sup>                                      |
| <br><b>EV(ClO<sub>4</sub>)<sub>2</sub></b><br><i>Angew. Chem. Int. Ed.</i> <b>2020</b> , <i>59</i> , 11533-11539. | 1.6 – 4.0        | 229                                       | 230, 210, 149 (0.1, 2, 5 C)                                    | 218/200/0.5 C   |
| <br><b>PVM</b><br><i>Chem. Sci.</i> <b>2020</b> , <i>11</i> , 10483-10487.                                       | 2.0 – 4.5        | 107                                       | 32, ~26 (1/2, 1 C)   | ~25/120/1 C   |
| <br><b>Phosphaviologen</b><br><i>Adv. Energy Mater.</i> <b>2016</b> , <i>6</i> , 1600944.                        | 1.8 – 3.2        | 77  | 60, 40, 35, 26 (1/3, 1.5, 3, 8 C)                              | 60/70/1 C   |
| <br><b>PVBVEtBr<sub>2</sub></b><br><i>J. Mater. Chem. A</i> <b>2022</b> , <i>10</i> , 10026-10032.               | 1.2 – 3.8        | 193                                       | 186, 157, 145, 133, 103, 77 (0.02, 0.04, 0.1, 0.2, 0.4, 1 A/g) | ~125/100/0.1 A g <sup>-1</sup>                                    |

|  |             |     |   |                              |
|--|-------------|-----|---|------------------------------|
|  <p><b>P3</b><br/><i>Chem Mater.</i> <b>2021</b>, <i>33</i>, 4596-4605.</p>                                     | 0.005 – 3.0 | 166 | 260, 180, 125, 90, 60<br>(0.2, 0.5, 1.0, 2.0, 5.0 A g <sup>-1</sup> )   | 110/1000/1 A g <sup>-1</sup> |
|  <p><b>(A2)<sup>2+</sup>Br<sub>2</sub></b><br/><i>Mater. Chem. Front.</i> <b>2023</b>, <i>7</i>, 3747-3753.</p> | 1.2 – 3.8   | 218 | 236, 216, 199, 186, 174<br>(0.2, 0.4, 0.6, 0.8, 1.0 A g <sup>-1</sup> ) | 227/3500/1 A g <sup>-1</sup> |

## References

- [S1] Lindström, H.; Södergren, S.; Solbrand, A.; Rensmo, H.; Hjelm, J.; Hagfeldt, A.; Lindquist, S.-E. Li<sup>+</sup> Ion Insertion in TiO<sub>2</sub> (Anatase). 2. Voltammetry on Nanoporous Films. *J. Phys. Chem. B* **1997**, *101*, 7717-7722.
- [S2] Liu, T. C.; Pell, W. G.; Conway, B. E.; Roberson, S. L. Behavior of Molybdenum Nitrides as Materials for Electrochemical Capacitors: Comparison with Ruthenium Oxide. *J. Electrochem. Soc.* **1998**, *145*, 1882-1888.
- [S3] (a) Luo, L.-W.; Ma, W.; Dong, P.; Huang, X.; Yan, C.; Han, C.; Zheng, P.; Zhang, C.; Jiang, J.-X. Synthetic Control of Electronic Property and Porosity in Anthraquinone-Based Conjugated Polymer Cathodes for High-Rate and Long-Cycle-Life Na–Organic Batteries. *ACS Nano* **2022**, *16*, 14590-14599. (b) Wang, Y.; Bai, P.; Li, B.; Zhao, C.; Chen, Z.; Li, M.; Su, H.; Yang, J.; Xu, Y. Ultralong Cycle Life Organic Cathode Enabled by Ether-Based Electrolytes for Sodium-Ion Batteries. *Adv. Energy Mater.* **2021**, *11*, 2101972. (c) Tao, R.; Zhang, T.; Tan, S.; Jafta, C. J.; Li, C.; Liang, J.; Sun, X.-G.; Wang, T.; Fan, J.; Lu, Z.; Bridges, C. A.; Suo, X.; Do-Thanh, C.-L.; Dai, S. Insight into the Fast-Rechargeability of a Novel Mo<sub>1.5</sub>W<sub>1.5</sub>Nb<sub>14</sub>O<sub>44</sub> Anode Material for High-Performance Lithium-Ion Batteries. *Adv. Energy Mater.* **2022**, *12*, 2200519.